Investigation of plasmonic resonances in the two-dimensional electron gas of an InGaAs/InP high electron mobility transistor

Justin W. Cleary*[a], Robert E. Peale[b], Himanshu Saxena[c] and Walter R. Buchwald[d]
[a]Solid State Scientific Corporation, Hollis, NH 03049
[b]Department of Physics, University of Central Florida, Orlando, FL 32816
[c]Zyberwear, Inc., Ocoee, FL 34761
[d]Air Force Research Laboratory / Sensors Directorate, Hanscom Air Force Base, MA 01731

ABSTRACT

The observation of THz regime transmission resonances in an InGaAs/InP high electron mobility transistor (HEMT) can be attributed to excitation of plasmons in its two-dimensional electron gas (2DEG). Properties of grating-based, gate-voltage tunable resonances are shown to be adequately modeled using commercial finite element method (FEM) software when the HEMT layer structure, gate geometry and sheet charge concentration are taken into account. The FEM results are shown to produce results consistent with standard analytical theories in the 10-100 cm^{-1} wavenumber range. An original analytic formula presented here describes how the plasmonic resonance may change in the presence of a virtual gate, or region of relatively high free charge carriers that lies in the HEMT between the physical grating gate and the 2DEG. The virtual gate and corresponding analytic formulation are able to account for the red-shifting experimentally observed in plasmonic resonances. The calculation methods demonstrated here have the potential to greatly aid in the design of future detection devices that require specifically tuned plasmonic modes in the 2DEG of a HEMT, as well as giving new insights to aid in the development of more complete analytic theories.

Keywords: plasmonics, infrared, terahertz, HEMT, 2DEG, detection

1. INTRODUCTION

Grating-coupled high electron mobility transistors (HEMTs) have potential for THz detection based on tunable plasmonic absorption modes[1]. The plasmons are excited optically in a two-dimensional electron gas (2DEG) layer via a conducting grating. This plasmonic resonance can be continuously tuned by changing the sheet charge density in the 2DEG, which is inherently controlled by the gate voltage of the device. These plasmonic modes are also determined by the materials in the HEMT and grating period. When the grating period is much less than the optical THz wavelengths, the grating will become polarized, generating local fields that enable the excitation of plasmons in the 2DEG.

Previous experiments[2-3] demonstrated transmission resonances in the region (THz frequencies) of expected plasmonic resonance devices for an InGaAs/InP HEMT. These experimental resonances however were red-shifted from expected analytical calculations while being obscured by Fabry-Perot oscillations and low optical transmission. The plasmonic resonance positions however were determined by a reduction in the quality factor, or increase in resonance width of these Fabry-Perot oscillations. Figure 1 (left) shows a schematic of the device while Fig. 1 (right) shows a cross-section of the layers in the actual HEMT being investigated. The device has a doped region in the InAlAs spacer layer. It was originally assumed that the charge carriers from the doped region fall into the quantum well of the 2DEG, which is typical of HEMT structures. If some charge carriers remain, however, this space with finite conductivity could act as a "virtual gate", which is physically closer to the 2DEG than the original gate, which is the metalized conducting grating. This virtual gate, first conceived in Ref. [3], adds complexity to the system.

Known analytic formulas[4-5] are able to predict plasmonic resonances in a typical HEMT, but are less accurate in more complicated structures. FEM simulations utilizing COMSOL Multiphysics are shown to be able to provide an accurate description of the plasmonic resonances of the typical HEMT structure. Also presented in this work are results relating observed red-shift to the presence of a virtual gate. A new analytic formulation is shown that accounts for the

* justin.cleary@hanscom.af.mil

presence of a virtual gate. FEM simulations (Silvaco Atlas) are completed to determine the amount of free charge carriers in the doped region of the HEMT indicating whether or not a virtual gate is present in the HEMT.

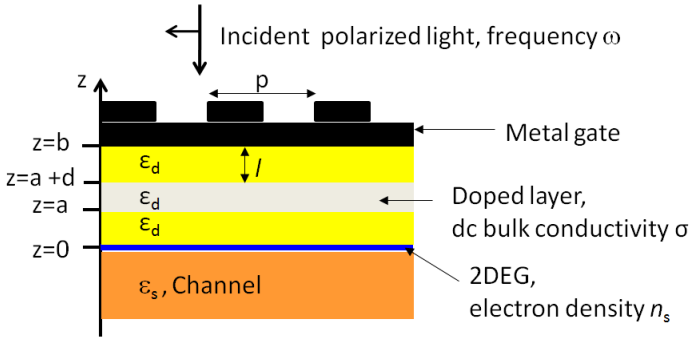

115nm	Ti/Au	
7.5 nm Ti		
20 nm $In_{0.52}Al_{0.48}As$ Undoped		
20 nm $In_{0.52}Al_{0.48}As$, $n_s = 4x10^{12}$ cm^{-2}		
4.5 nm $In_{0.52}Al_{0.48}As$ Undoped		
40 nm $In_{0.53}Ga_{0.47}As$ Channel		
300 nm $In_{0.52}Al_{0.48}As$ Buffer Undoped		
InP Substrate		

Figure 1. Schematic (left) and structure (right) of the HEMT.

2. THEORY

An analytical formula is now seemingly well known for the excitation of plasmons in a 2DEG by the local fringing fields of a polarized, metalized grating. The plasmon resonance frequency is[4]

$$\omega_p(z) = \sqrt{\frac{n_s e^2}{m^*}\frac{q}{\varepsilon_o\left[\varepsilon_s + \varepsilon_d Coth(qz)\right]}}, \tag{1}$$

where ε_t and ε_d are the relative permittivities of the barrier layer and channel, respectively, as seen in Fig. 1, q is the plasmon wavevector and z is the distance from the gate to the 2DEG, or b, in Fig. 1. The sheet charge density of the 2DEG, or n_s, is proportional to the applied gate voltage while depending on other material parameters. The plasmon wavevector is $2\pi m/p$ where m is the integer resonance order. The condition for plasmon excitation in the 2DEG is that the normally incident wavevector must have an optical frequency that matches that of Eq. 1 with the grating period also being much less than the incident wavelength, as stated earlier. Eq. 1 assumes the case of the typical HEMT, which has no virtual gate.

A different dispersion relation can be derived for the plasmonic resonance in a HEMT in the presence of a virtual gate. This plasmon resonance frequency can be found by solving[6]

$$\left(\varepsilon_d \cosh(qb) + \varepsilon_s \sinh(qb)\right)\left(\omega^2 - \omega_p^2(b)\right) + \frac{i\sigma \sinh(ql)\sinh(qd)}{\varepsilon_d \varepsilon_0 \omega}\left(\varepsilon_d \cosh(qa) + \varepsilon_s \sinh(qa)\right)\left(\omega^2 - \omega_p^2(a)\right)$$

$$-\frac{\sinh(qd)\cosh(ql)}{1 - i\varepsilon_d \varepsilon_0 \omega/\sigma}\left(\varepsilon_d \sinh(qa) + \varepsilon_s \cosh(qa)\right)\left(\omega^2 - \frac{\varepsilon_d \coth(qa) + \varepsilon_s}{\varepsilon_d \tanh(qa) + \varepsilon_s}\omega_p^2(a)\right) = 0 \tag{2}$$

for the optical frequency ω. ω_p in this relationship is the plasmon frequency found by Eq. 1, with the specified parameter distance in parentheses substituted for z. This quartic relationship is of the form

$$A\omega^4 + B\omega^3 + C\omega^2 + D\omega + E = 0, \tag{3}$$

where the coefficients can be found by

$$F1 = \varepsilon_d \cosh(qb) + \varepsilon_s \sinh(qb), \tag{4}$$

$$F2 = \frac{i\sigma \sinh(ql)\sinh(qd)}{\varepsilon_d \varepsilon_0}, \tag{5}$$

$$F3 = \varepsilon_d \cosh(qa) + \varepsilon_s \sinh(qa), \tag{6}$$

$$F4 = -\sinh(qd)\cosh(ql), \tag{7}$$

$$F5 = -i\varepsilon_d \varepsilon_0 / \sigma, \tag{8}$$

$$F6 = \varepsilon_d \sinh(qa) + \varepsilon_s \cosh(qa), \tag{9}$$

$$F7 = \frac{\varepsilon_d \coth(qa) + \varepsilon_s}{\varepsilon_d \tanh(qa) + \varepsilon_s}, \tag{10}$$

$$A = (F1)(F5), \tag{11}$$

$$B = F1 + (F2)(F3)(F5) + (F4)(F6), \tag{12}$$

$$C = -(F1)(F5)\omega_p{}^2(b) + (F2)(F3), \tag{13}$$

$$D = -(F1)\omega_p{}^2(b) - (F2)(F3)(F5)\omega_p{}^2(a) - (F4)(F6)(F7)\omega_p{}^2(a), \tag{14}$$

and

$$E = -(F2)(F3)\omega_p{}^2(a). \tag{15}$$

The solution for the modified plasmon frequency from the quartic equation is

$$\omega = -\frac{B}{4A} + \frac{W + \sqrt{-\left(3\alpha + 2y + 2\delta / W\right)}}{2}, \tag{16}$$

where

$$\alpha = -\frac{3B^2}{8A^2} + \frac{C}{A}, \tag{17}$$

$$\delta = \frac{B^3}{8A^3} - \frac{BC}{2A^2} + \frac{D}{A}, \tag{18}$$

$$\gamma = -\frac{3B^4}{256A^4} + \frac{CB^2}{16A^3} - \frac{BD}{4A^2} + \frac{E}{A}, \tag{19}$$

$$P = -\frac{\alpha^2}{12} - \gamma, \tag{20}$$

$$T = -\frac{\alpha^3}{108} + \frac{\alpha\gamma}{3} - \frac{\delta^2}{8}, \tag{21}$$

$$R = -\frac{T}{2} + \sqrt{\frac{T^2}{4} + \frac{P^3}{27}}, \tag{22}$$

$$U = \sqrt[3]{R} \quad , \tag{23}$$

$$y = -\frac{5}{6}\alpha + U - \frac{P}{3U} \quad if\ U \neq 0, \tag{24}$$

and

$$W = \sqrt{\alpha + 2y}. \tag{25}$$

The quartic equation, of course, has four solutions. The correct solution will reproduce the dispersion relationship in Eq. 1 in the limit of the virtual gate region becoming infinitely thin (*d* approaches 0) and the limit of the virtual gate region

being moved to the physical position of the actual gate (*a* approaching *b*). Eq. 16 gives the solution to the quartic (Eq. 2) that satisfies these limits.

3. RESULTS

FEM analysis using COMSOL Multiphysics was used to demonstrate the plasmonic effects expected in the 2DEG of the HEMT. The structure shown in Fig. 1 (right) was programmed with polarized THz light being incident normal to the surface. Figure 2 shows a screenshot of the simulation result, demonstrating the grating polarization required for excitation of plasmons in the 2DEG. The grating period is 500 nm, which is much less than the optical wavelength (in this case 50 μm), with a duty cycle of 80%.

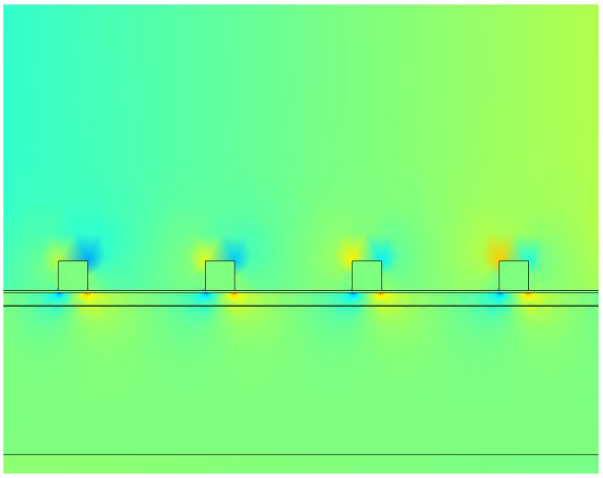

Figure 2. COMSOL screenshot demonstrating polarized gratings.

The HEMT in the COMSOL simulation was constructed according to the structure of Figure 1 with no doping in the InAlAs region, or more specifically, there is no virtual gate. ε_d was taken to be 12.24 for InAlAs, while ε_s was taken to be 13.65 for InGaAs[2]. To simplify the calculations, the metallic gate region was assumed to be made entirely of gold, with the Drude model being used for the permittivity. The 2DEG was modeled as a 3 nm thick layer of InGaAs (as the 2DEG will lie within the channel region) with the appropriate Drude conductivity and permittivity as determined by the sheet charge density. The 2DEG lies 44.5 nm from the gating gate, as shown in Fig. 1. The two simulated variables are the incident wavelength and the sheet charge density in the 2DEG. The wavelength range was set to show expected plasmonic modes. Three specific values of sheet charge density were used, corresponding to previously determined analytic results[2]. These values are n_s = 4.6, 3.0, and 1.5 × 10^{11} cm^{-2}, which corresponds to gate voltages of 0, -0.1, and -0.2 V respectively.

Figure 3 presents COMSOL results showing plasmonic modes in the 2DEG for the zero gate voltage setting. The incident frequencies are 54.7, 90.3, and 115.5 cm^{-1} (182.8, 110.8, and 86.6 μm) for the first through third resonance orders, respectively. The first order modes have period approximately equal to that of the grating period, with higher orders having this period multiplied by its respective integer order. The non-zero gate voltage settings resulted in similar plasmonic modes, shifting to lower frequencies for smaller values of sheet charge density, as expected from Eq. 1.

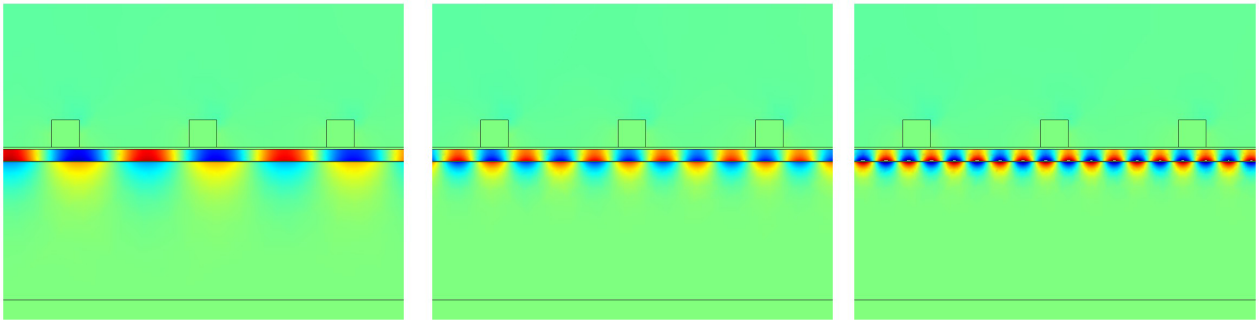

Figure 3. COMSOL-simulated plasmonic modes at incident frequencies of 54.7, 90.3, and 115.5 cm^{-1} (left to right) with zero gate voltage. The plasmon resonance orders one through three respectively.

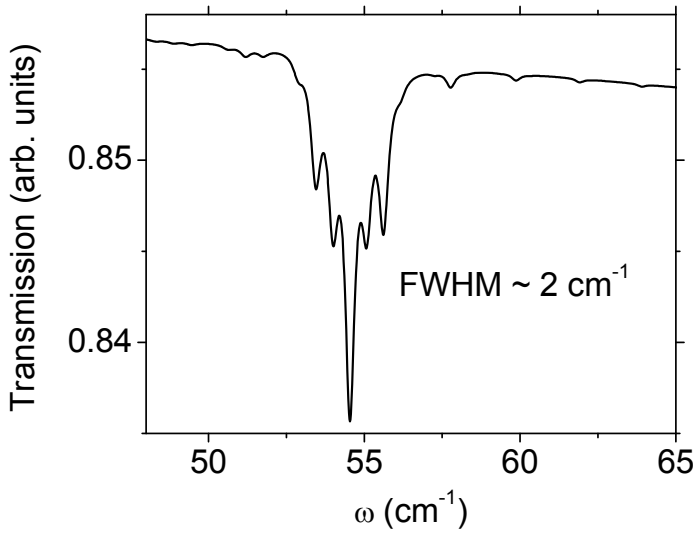

Figure 4: COMSOL transmission simulation illustrating the first order resonance with zero gate voltage.

Figure 4 presents COMSOL results showing the first order transmission resonance of the HEMT with zero gate voltage applied. The transmission is calculated from integrating over the normalized electric field in the substrate region of the HEMT and dividing by the same normalized electric field when no grating structure is present. At frequencies between those pictured in Fig. 3, the plasmonic modes dissipate as seen by the increase in transmission on either side of the resonance in Fig. 4. The observed line-width of ~ 2 cm^{-1} is comparable with the line-width predicted by analytical methods[2]. The COMSOL results show oscillations that appear within the plasmonic resonance. It should be noted however that the COMSOL simulation completed here has a grating gate region of length 10 μm which is an order of magnitude smaller than the actual grating gate length used in previous experiments[2] and two orders of magnitude less than the optical wavelength. These oscillations are likely an apodization effect caused by having a short grating that terminates abruptly at either end. Due to the observed anomalous line-shape in the FEM simulation, analytical models, such as Ref. [5], are still better suited for prediction of plasmonic line shapes in the optical transmission of HEMTs.

Figure 5 presents the plasmon frequencies determined from the COMSOL simulations, along with calculations obtained directly from Eq. 1. Separate curves are plotted for three resonance orders. The COMSOL results fall very nearly on the curved predicted by the basic plasmonic 2DEG theory. Increasing the sheet charge density in the 2DEG increases the plasmonic resonance frequency, as both results show. This result shows proof of principle that COMSOL can accurately predict plasmonic modes in a 2DEG if the structure is accurately depicted.

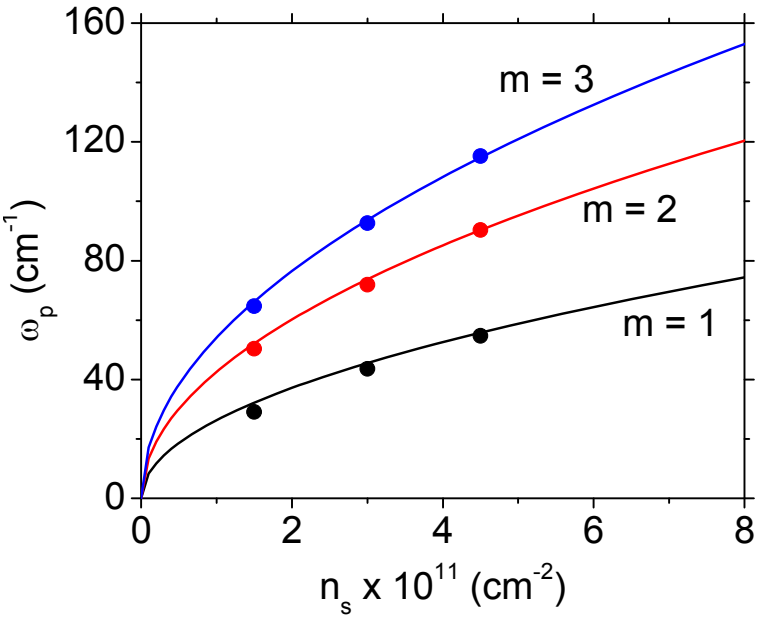

Figure 5. Plasmonic resonance frequencies as a function of sheet charge density in the 2DEG from COMSOL (scatter points) and Eq. 1 (solid curves) for three resonance orders.

The Silvaco Atlas 2-D device simulator (FEM analysis software) was used to determine the free carrier concentration profile with the doping layer having a carrier concentration of 2×10^{18} cm^{-3}, as specified by the manufacturer (Fig. 1). Figure 6 presents the electron concentration throughout the device. The dashed lines indicate the various regions of the device according to Fig. 1. An electron concentration of 10^{19} cm^{-3} is found in the 2DEG, with an order of magnitude decrease within ~ 3 nm (the thickness estimated in the COMSOL simulations). A more interesting result of the Silvaco simulation is that the original donor region still maintains a peak electron concentration of 10^{17} cm^{-3}. This high of a free carrier concentration indicates that the virtual gate theory for this specific HEMT device may be valid.

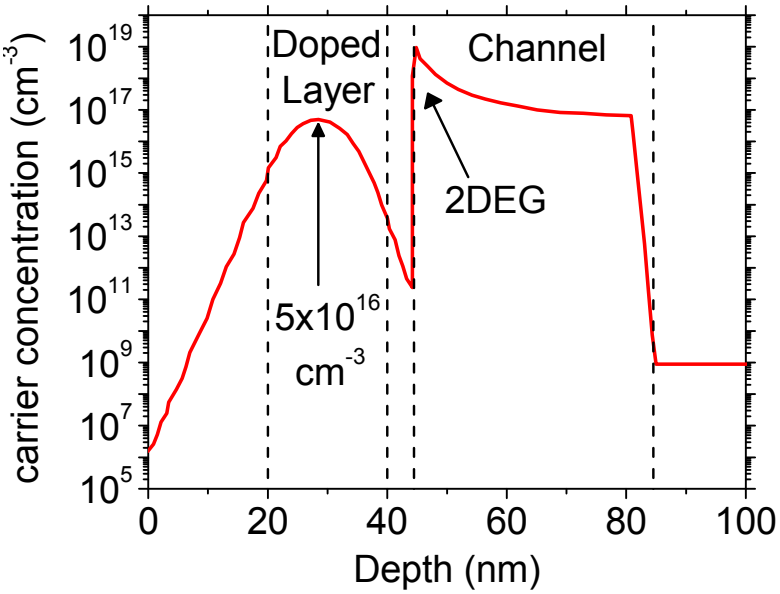

Figure 6. FEM results giving the electron carrier concentration throughout the HEMT profile. The doping in the InAlAs layer is 2×10^{18} cm^{-3}.

With the possibility of a virtual gate being realized for this device, analytic simulations are now shown utilizing the quartic equation (Eqs. 2-25). Figure 7 presents experimental data[2] (scatter points) with fittings based on the quartic solution (solid curves). The fitting parameters used are the finite conductivity of the virtual gate, σ, and the sheet charge density of the 2DEG. The fittings give a fairly accurate description of the data, with the exception of the 3rd order resonance for the -0.2 gate voltage. It is noted that the experimental resonances may have error within a few wavenumbers due to the lack of clear, distinguishable resonances.

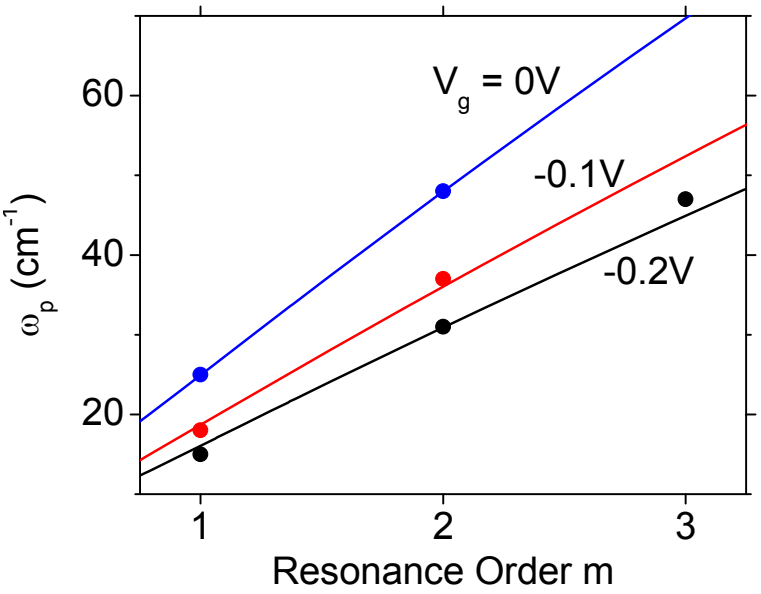

Figure 7. Experimental data[2] (scatter points) and quartic fittings using Eqs. 2-25 (solid curves) of plasmonic resonance frequencies as a function of the plasmonic integer resonance order for three gate voltages.

Table 1 presents results of fitting the experimental data with the quartic solution. The sheet charge density compares well with published analytic values which were determined for the same HEMT at a temperature of 22 K. The experiments were most likely at temperatures above 12 K, possibly even being near 22 K. Both n_s and σ decrease as a function of gate voltage, indicating that both the 2DEG and the virtual gate are being depleted of charge carriers. Also shown in Table 1 are the complex plasmonic resonance frequency solutions obtained from the fittings for the three resonance orders observed. The real parts correspond to the scatter points seen in Fig. 7. It is noted that the relatively large imaginary components may play a role in the absence of well defined resonances in the experimental data[2].

Table 1. Parameters determined from the fitting in Fig. 7 compared with those from analytic results[2].

	Vg = 0V	**-0.1V**	**-0.2V**
n_s Published [cm^{-2}]	4.6×10^{11}	3.0×10^{11}	1.5×10^{11}
n_s Fitting [cm^{-2}]	5.3×10^{11}	3.0×10^{11}	2.2×10^{11}
σ Fitting [1/Ω-cm]	550	450	350
$\omega_{m=1}$ [cm^{-1}]	25.0-8.2i	18.7-5.6i	16.1-5.4i
$\omega_{m=2}$ [cm^{-1}]	47.9-7.2i	36.0-5.0i	30.9-4.7i
$\omega_{m=3}$ [cm^{-1}]	-	-	44.9-4.5i

The conductivity can be related to the carrier mobility by

$$\mu = \sigma / Ne\,, \tag{26}$$

where N is the charge carrier density in the doped $In_{0.52}Al_{0.48}As$ layer, as determined by the FEM calculations (Fig. 6). For the zero gate voltage conductivity from the fittings (Table 1) and a carrier concentration of 5×10^{16} cm^{-3}, the mobility is ~7×10^{4} cm^2/Vs. This value is an order of magnitude larger than what is expected for $In_{0.52}Al_{0.48}As$ with this doping[7-9].

Silvaco Atlas was again utilized for the same HEMT structure; however, this time a doping concentration of 2.8×10^{18} cm^{-3} was used for the InAlAs layer. Figure 8 presents this new charge carrier profile of the HEMT. The peak in the virtual gate region for this larger doping concentration is 1×10^{18} cm^{-3}. Using Eq. 26 with this value and zero gate voltage conductivity gives a mobility $\sim3\times10^{3}$ cm^2/Vs. This mobility is of the same order as the expected mobility for $In_{0.52}Al_{0.48}As$ with this doping[7-9]. This leads to the possibility of the original specified doping of the HEMT being inaccurate by up to ~30%. Higher mobility is, however, expected for the low temperatures of the original experiments, indicating that the doping may have been some intermediate value between those used in the two Silvaco FEM simulations. It is noted that without accurate knowledge of the electron concentration profile in the HEMT, COMSOL FEM simulations do not provide an accurate description of the plasmonic resonances.

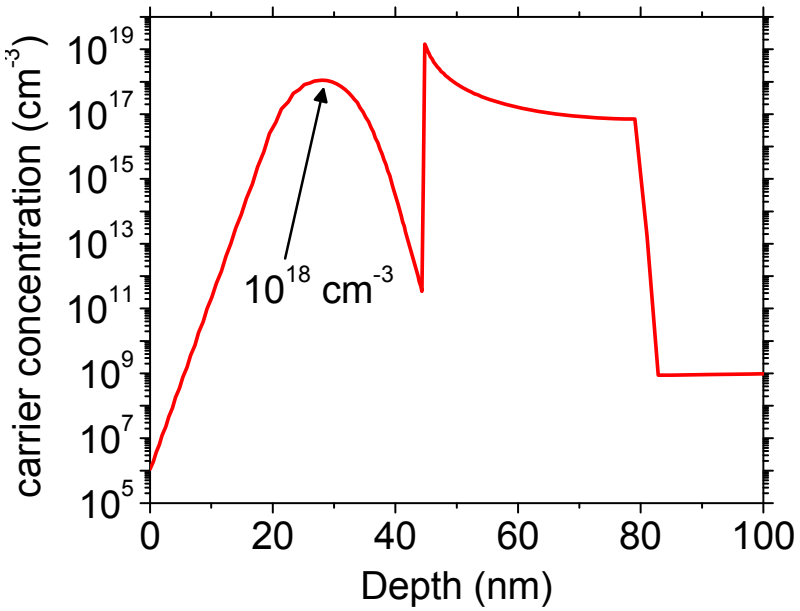

Figure 8. FEM results giving the electron carrier concentration throughout the HEMT profile. The doping in the InAlAs layer is 2.8×10^{18} cm^{-3}.

4. SUMMARY

This paper reports on analytic and numerical results for an InGaAs/InP HEMT. FEM analysis results for the HEMT structure indicate that plasmonic resonances coincide well with the known analytic formula for plasmons in a 2DEG. This is proof of principal that this method can be used to further predict plasmon resonances when the structure is accurately known although thus far analytical methods may still be better suited for determining transmission resonance line-shapes. An original analytic formula describes how the plasmonic resonance may change when a virtual gate is present, or region of relatively high free charge carriers that lies between the physical grating gate and the 2DEG. FEM analysis for the InGaAs HEMT structure indicates a high free carrier concentration in the doped region of the HEMT, which leaves the virtual gate theory as viable. This virtual gate and analytic formulation are able to account for the shifting in plasmonic resonances to lower frequencies, as previously observed experimentally. The formulation presented here may be further used in similar structures where some charge carriers remain in the doped region of the HEMT.

ACKNOWLEDGMENTS

JWC and WRB would like to acknowledge support from the Air Force Office of Scientific Research (Program Manager Dr. Gernot Pomrenke) under contract number 09RY09COR. REP acknowledges support also by the Air Force Office of Scientific Research (Program Manager Dr. Gernot Pomrenke) under grant number FA95501010030.

REFERENCES

[1] Peralta, X. G., Allen, S. J., Wanke, M. C., Harff, N. E., Simmons, J. A., Lilly, M. P., Reno, J. L., Burke, P. L., and Eisenstein, J. P., "Terathertz photoconductivity and plasmon modes in double-quantum-well field-effect transistors," Appl. Phys. Lett., 81, 1627-1629 (2002).

[2] Saxena, H., Peale, R. E., Buchwald, W. R., "Tunable two-dimensional plasmon resonances in an InGaAs/InP high electron mobility transistor," J. Appl. Phys., 105, 113101 (2009).

[3] Peale, R. E., Saxena, H., Buchwald, W. R., Aizin, G., Muravjov, A. V., Veksler, D. B., Pala, N., Hu, X., Gaska, R., and Shur, M. S., "Grating-gate tunable plasmon absorption in InP and GaN based HEMTs," Proc. SPIE 7467, 74670Q (2009).

[4] Allen, S. J., Tsui, D. C., and Logan, R. A., "Observation of the two-dimensional plasmon in silicon inversion layers," Phys. Rev. Lett., 38, 980-983 (1977).

[5] Zheng, L., Schaich, W. L., and MacDonald, A. H., "Theory of two-dimensional grating couplers," Phys. Rev. B., 41, 8493-8499 (1990).

[6] Aizin, G., personal communication, 2009.

[7] Tanahashi, T., Nakajima, K., Yamaguchi, A., and Umebu, I., "Electrical properties of undoped and Si-doped $Al_{0.48}In_{0.52}As$ grown by liquid phase epitaxy," Appl. Phys. Lett., 43, 1030-1032 (1983).

[8] Bhattacharyya, A., Chattopadhyay, D., and Ghosal, A., "Electron mobility of $Al_{0.48}In_{0.52}As$," Phys. Rev. B, 31, 2524-2525 (1985).

[9] Goto, S., Ueda, T., Ohshima, T., and Kakinuma, H., "Effect of growth conditions on Si doping into InAlAs grown by metal-organic vapor phase epitaxy," 10th Intern. Conf. on Indium Phosphide and Related Materials, 119-122 (1998).